

Article

Adsorption of Diphenolic Acid from Contaminated Water onto Commercial and Prepared Activated Carbons from Wheat Straw

Raid Alrowais ^{1,*}, Noha Said ², Muhammad Tariq Bashir ³, Ahmed Ghazy ⁴, Bandar Alwushayh ¹
and Mahmoud M. Abdel Daiem ^{2,5}

¹ Department of Civil Engineering, College of Engineering, Jouf University, Sakakah 72388, Saudi Arabia
² Environmental Engineering Department, Faculty of Engineering, Zagazig University, Zagazig 44519, Egypt
³ Department of Civil Engineering, CECOS University of IT and Emerging Sciences, Peshawar 25000, Pakistan
⁴ Department of Mechanical Engineering, College of Engineering, Jouf University, Sakakah 72388, Saudi Arabia
⁵ Civil Engineering Department, College of Engineering, Shaqra University, Al-Duwadmi 11911, Saudi Arabia
* Correspondence: rnalrowais@ju.edu.sa; Tel.: +966-502-229-973

Abstract: The fabrication of carbon materials from biomass residues can be a promising economical approach for absorbing various target pollutants from aqueous phase. In the study, the adsorption of diphenolic acid (DPA) is investigated on activated carbons fabricated from wheat straw (ACWS) and commercial-activated carbon cloth (CACC). Adsorption kinetics, isotherms, and operational variables (solution pH and ionic strength) are analyzed for the adsorption capacity of the DPA on both carbons. The results show that the ACWS has a higher surface area (1164 m²/g) and volume of micropores (0.51 cm³/g) than those of the CACC. The second-order kinetics model fitted the experiment data better than the first kinetics models with a lower percentage of deviation. The adsorption capacity of the ACWS (264.90 mg/g) is higher than the CACC (168.19 mg/g) because of the higher surface area and volume of micropores of the ACWS. The adsorption isotherm shows that the adsorption of the DPA on the ACWS and CACC is consistent with the Langmuir and Freundlich isotherm models, respectively. The pH has a significant effect on DPA adsorption onto both carbons. The adsorption process is favored at the acidic pH, but the presence of electrolytes has no effect on the adsorption capacity of both carbons due to the screening effect. Thus, the preparation of activated carbon from wheat straw is an attractive option to recycle the wheat straw to added-value materials that can be used for the removal of such pollutants from aqueous solution. These findings can increase the research knowledge about the management of different straws in a sustainable way to produce activated carbon for different applications.

Keywords: adsorption; activated carbon; wheat straw; diphenolic acid; carbon cloth



Citation: Alrowais, R.; Said, N.; Bashir, M.T.; Ghazy, A.; Alwushayh, B.; Daiem, M.M.A. Adsorption of Diphenolic Acid from Contaminated Water onto Commercial and Prepared Activated Carbons from Wheat Straw. *Water* **2023**, *15*, 555. <https://doi.org/10.3390/w15030555>

Academic Editors: Amimul Ahsan and Monzur Imteaz

Received: 3 January 2023

Revised: 25 January 2023

Accepted: 28 January 2023

Published: 31 January 2023



Copyright: © 2023 by the authors. Licensee MDPI, Basel, Switzerland. This article is an open access article distributed under the terms and conditions of the Creative Commons Attribution (CC BY) license (<https://creativecommons.org/licenses/by/4.0/>).

1. Introduction

Many synthetic chemical compounds are currently used throughout the world and, depending on their application, many of them are continuously accumulated in urban landfills [1,2]. The low biodegradability that they can present causes their gradual appearance in the composition of the leachates that are produced in solid waste deposits, which, in turn, causes a serious environmental problem that requires correct handling and treatment [3]. Organic pollutants detected in the composition of landfill leachate and different water types; one such pollutant is diphenolic acid (DPA) [4,5], which is an endocrine disruptor [6]. Moreover, more attention has been paid to replacing bisphenol A (BPA) with DPA in the fabrication of polyesters, due to its lower price compared to BPA with the same function [7]. Unfortunately, DPA has the same effect as BPA on the environment and has been associated with cancer, liver damage, and obesity epidemic [8].

Few studies have investigated the degradation or elimination of DPA from polluted water via photo-oxidation and adsorption processes. Abdel Daiem et al. [6] investigated the degradation of DPA by using gamma radiation, and they found that the degradation

rate increased at higher irradiation, and there was a slight dependence on the dose rate and a major influence of pH on the degradation rate. Abdel Daiem et al. [5] investigated the single and competitive adsorption of DPA and BPA onto two commercial-activated carbons (ACs). The results showed that the both ACs have a lower adsorption capacity for DPA than for BPA that maybe related to the contaminant molecular size and chemical characteristics of the contaminant and adsorbents. Furthermore, the amount of BPA and DPA in competitive adsorption showed a decrease by 50% and 70% for BPA and DPA, respectively. Guo et al. [9] studied the removal of DPA under ultra-violet (UV) radiation in the presence of β -cyclodextrin (β -CD), reported its enhancement in the presence of β -CD. Guo et al. [10] studied the photochemical remediation of DPA in the absence of β -CD and TiO_2 and found the presence of TiO_2 improves the removal ratio, basically due to the adsorption of DPA on the TiO_2 surface. Abdel Daiem et al. [11] investigated the adsorption of DPA onto rice straw-activated carbon and the results showed that the fabricated AC using ZnCl_2 (RSZ) and H_3PO_4 (RSP) has a slight surface area of $771 \text{ m}^2/\text{g}$ and $613 \text{ m}^2/\text{g}$, respectively, meanwhile, the adsorption capacity was higher in case of RSZ than that of RSP.

The removal of DPA from aqueous solution can be efficiently addressed by means of different technologies such as physicochemical, biological, and advanced oxidation reduction processes (AORPs) [2]. The highest yields were detected for the removal of DPA or a similar contaminant by using the physicochemical processes [2]. The adsorption process onto ACs are considered one of the most reliable and effective physicochemical processes for the treatment of water and wastewater, achieving a higher reduction in organic and inorganic contaminants in comparison to other methods [2,11]. Moreover, it has many advantages such as cheap technology, low energy consumption, and its ability to remove the contaminant from aqueous solution, and there are no by-products or new generated contaminants such as other processes. Furthermore, this process is considered a very important treatment that can be applied at the end of the water or wastewater treatment plants. Since the soluble compound to be removed must be concentrated on the surface of the carbon material, a determining parameter of the process will be the high surface area of the carbon material. Currently, the carbon material universally used as an adsorbent in water treatment is AC, due to its greater capacity for the extraction of organic and inorganic compounds that have not been completely treated. ACs are materials that have a high adsorption power; as a result, among other characteristics, they have an important and varied network of pores. The AC can be defined as a material that has been manufactured from a raw material (lignocellulosic residue) with a high carbon content and that develops its porosity through a specific activation process in different applications [11–14]. In consequence, the fabrication of ACs from lignocellulosic biomass residues is considered an attractive option from an environmental point of view, where it is a recycling option for those residue and solve their disposal problems, as well as produce ACs that have a high potential to remove pollutants from aqueous solutions. Moreover, the saturated ACs fail to be reused and are landfilled or incinerated. It can be regenerated by different methods that make it a suitable material for multiple adsorption [15]. Thus, making activated carbon from renewable resources such as waste biomass is more intriguing because it is sustainable [16].

The quantity of biomass residues is considered very high in different countries [17–19]. The conversion of these residues to added-value materials could be used in different applications [11,13,20–22]. Previous studies investigated the fabrication of ACs from different biomass residues and the factors affecting production and adsorption mechanism [23–27]. Wheat straw is considered one of the highest biomass residues in different countries [28]. Moreover, few studies have investigated converting the wheat straw to activated carbons [29,30]. Ma [30] investigated preparing ACs from wheat straw via ZnCl_2 and KOH to remove methylene blue (MB) from aqueous solution. He demonstrated that ZnCl_2 -AC had a higher surface area, more micropores, developed an aromatic structure and high adsorption capacity (265.96 mg/g) in comparison to that via KOH (146.84 mg/g).

Moreover, the regeneration efficiency was higher than 70% after five regeneration cycles. Mao et al. [29] prepared activated carbon from pinewood and wheat straw by KOH and microwave heating. They found that ACs from pinewood and wheat straw have high surface areas of 2044 and 1250 m²/g, respectively.

From this background, the studies that investigated the adsorption of DPA from contaminated water are very limited. Thus, the main objective of this work is to investigate the adsorption of DPA from aqueous phase onto commercial and fabricated activated carbons from wheat straw. Moreover, the adsorption kinetics, isotherms, and the influence of the solution pH and ionic strength on the adsorption of DPA will be studied to determine the adsorption mechanism.

2. Material and Methods

Figure 1 illustrates the methodology of the current study. It includes details about the characterization of wheat straw and DPA, the fabrication of activated carbon from wheat straw (ACWS) and the characterization of carbons and adsorption process.

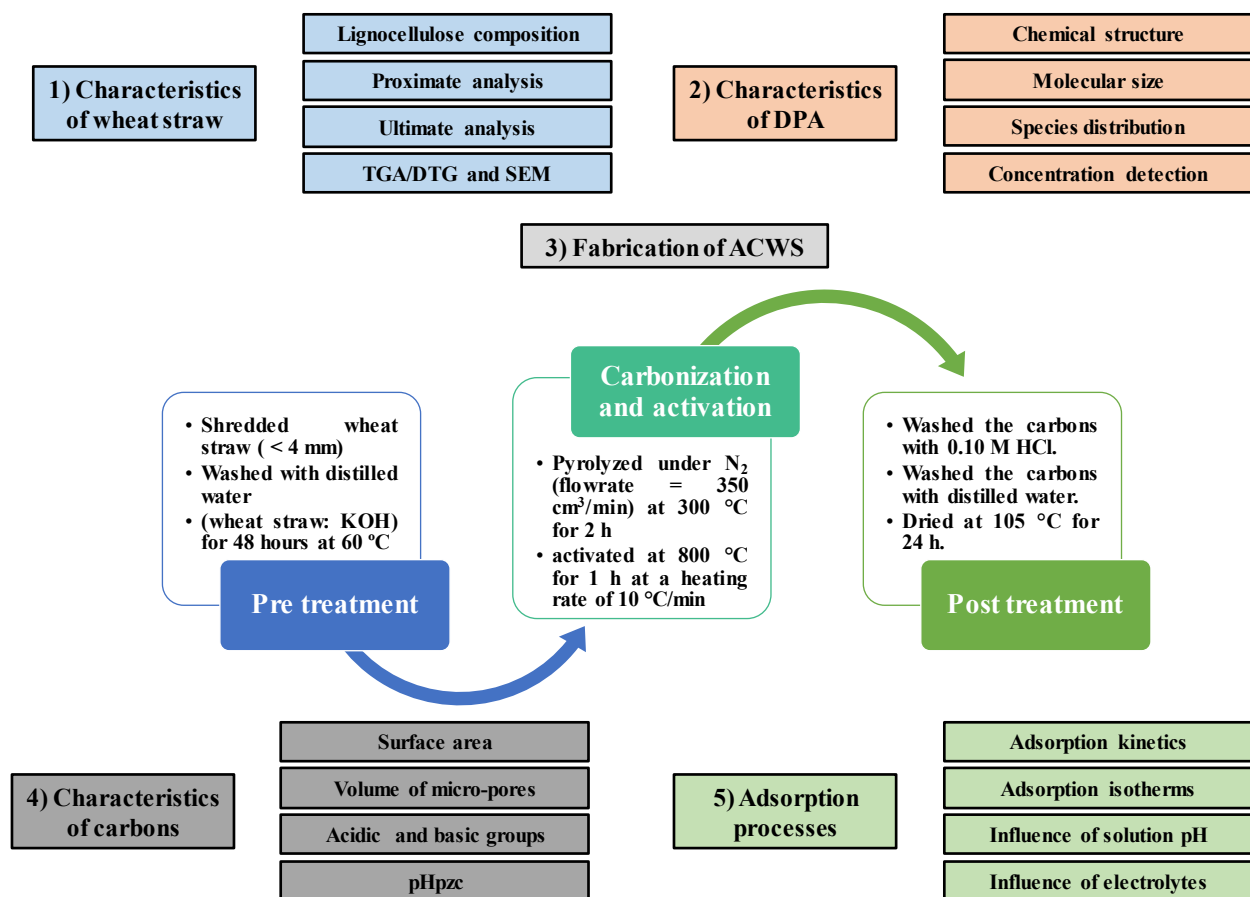


Figure 1. Research methodology for the preparation of carbon and the adsorption of DPA onto activated carbon.

2.1. Reagents

All chemical reagents used in this study (diphenolic acid, sodium chloride, sodium hydroxide, potassium hydroxide, hydrochloric acid, and silver nitrate) were high purity analytical grade reagents supplied by Sigma-Aldrich. All solutions were prepared with ultrapure water obtained from Milli-Q[®] equipment (Millipore). Table 1 presents physico-chemical properties of DPA that were calculated by using ChemIDplus advanced database. Figure 2 depicts the species distribution, chemical structure, and molecule size of DPA.

Concentrations of DPA were determined by UV-visible spectrophotometer (DRB200 Reactor 1 Block 9 × 16 MM/2 × 20 MM) at a wavelength 279 nm.

Table 1. Physicochemical properties of DPA.

	Molecular Weight (g/mol)	V_A ^(a) (cm ³ /mol)	S ^(b) (g/L)	log K_{ow} ^(c)	pKa ₁ ^(d)	pKa ₂ ^(e)	pKa ₃ ^(f)
DPA	286.33	315	0.40	3.58	4.66	9.70	10.45

Note(s): ^(a) Liquid molar volume at the normal boiling point. ^(b) Solubility in water. ^(c) Log octanol-water partition coefficient. ^(d-f) Corresponding to the successive deprotonations.

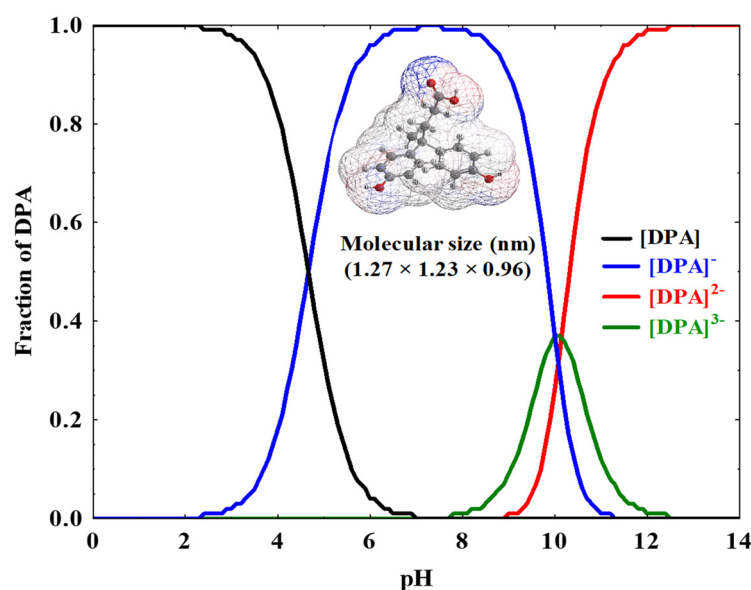


Figure 2. Species distribution, chemical structure, and molecule size of DPA.

2.2. Adsorbent Materials

The prepared ACWS and commercial-activated carbon cloth (CACC) were used in this study. The raw wheat straw samples were collected from Al-dawadmi, Saudi Arabia. The lignocellulose composition, proximate analysis, ultimate analysis, thermogravimetric analysis (TGA and DTG) and scanning electron microscopy (SEM) of wheat straw samples were investigated according to previous studies [13,31].

The ACWS was prepared from wheat straw samples, which were shredded into a small size (<4 mm) then washed to remove any impurities with distilled water and dried at 105 °C. The dried samples were mixed with KOH with impregnation ratio (1:1) by weight (wheat straw: KOH) for 48 h at 60 °C. Then they were pyrolyzed under N₂ (flowrate = 350 cm³/min) at 300 °C for 2 h and then activated at 800 °C for 1 h at a heating rate of 10 °C/min. The obtained ACWS was washed with 0.10 M HCl to remove KOH, then the samples were washed with distilled water until the chloride ions were no longer detected by using AgNO₃ solution. The washed samples were then dried at 105 °C for 24 h.

Both the ACWS and CACC samples were chemically and texturally characterized, recording the surface area, pore size distribution, oxygen surface groups, and pH of the point of zero charge (pH_{pzc}). A detailed description for the measurement procedures was previously reported [32].

2.3. Adsorption Processes

2.3.1. Adsorption Kinetics

The adsorption kinetics of DPA on the ACWS and CACC samples were investigated by adding 100 mg of carbon in 0.20 L Erlenmeyer flasks containing 25, 50, and 100 mg/L of

the initial concentration of DPA. The solution pH was kept in natural condition without any addition. More details about the kinetics processes were described in previous study [2]. The adsorption kinetic models frequently used are represented as the first- and second-order kinetic equations shown in Equations (1) and (2).

$$q = q_{\text{pred},1} \left(1 - e^{-k_1 t}\right) \quad (1)$$

$$q = \frac{q_{\text{pred},2}^2 k_2 t}{1 + q_{\text{pred},2} k_2 t} \quad (2)$$

where q : mass of adsorbate adsorbed, mg/g, $q_{\text{pred},1}$: mass of adsorbate adsorbed predicted from the first-order kinetic model, mg/g, $q_{\text{pred},2}$: mass of adsorbate adsorbed predicted from the second-order kinetic model, mg/g, k_1 : the rate constant of the first-order kinetic model, L/h, k_2 : the rate constant of the second-order kinetic model, g/mg/h, and t : time, min.

Equation (3) is used to calculate the average absolute percentage deviations for both kinetics models.

$$\%D = \frac{1}{N} \sum_{i=1}^N \left| \frac{q_{\text{exp}} - q_{\text{pred}}}{q_{\text{pred}}} \right| \times 100\% \quad (3)$$

where %D: percentage of deviation, N: number of points, q_{exp} : mass of adsorbate adsorbed experimentally, mg/g, and q_{pred} : mass of adsorbate adsorbed predicted, mg/g.

2.3.2. Adsorption Isotherm

The adsorption isotherms on carbon samples were performed by using different initial concentrations of DPA (50, 100, 200, 300, 400, and 500 mg/L). To determine the adsorption type and mechanism, Equations (4) and (5) represent the Langmuir and Freundlich adsorption isotherm models that are considered the most widely used models for adsorption process:

$$X_{\text{eq}} = \frac{BX_m C_e}{1 + BC_e} \quad (4)$$

$$X_{\text{eq}} = K_F C_e^{1/n_F} \quad (5)$$

where X_{eq} : quantity adsorbate adsorbed per unit mass of adsorbent (mg/g), X_m : adsorption capacity (mg/g), B : Langmuir constant (L/mg), C_e : concentration of adsorbate at equilibrium (mg/L), $1/n_F$: sorption intensity or surface heterogeneity, and K_F : relative adsorption capacity.

2.3.3. Operational Parameters

There are different variables that were investigated on the adsorption isotherm such as the solution pH (3, 5, 6, 8, and 10) and the presence of electrolytes (0, 0.0001, 0.001, and 0.01 M of NaCl) at the initial concentration of DPA 500 mg/L at ambient temperature 25 °C.

3. Results and Discussion

3.1. Wheat Straw Characteristics

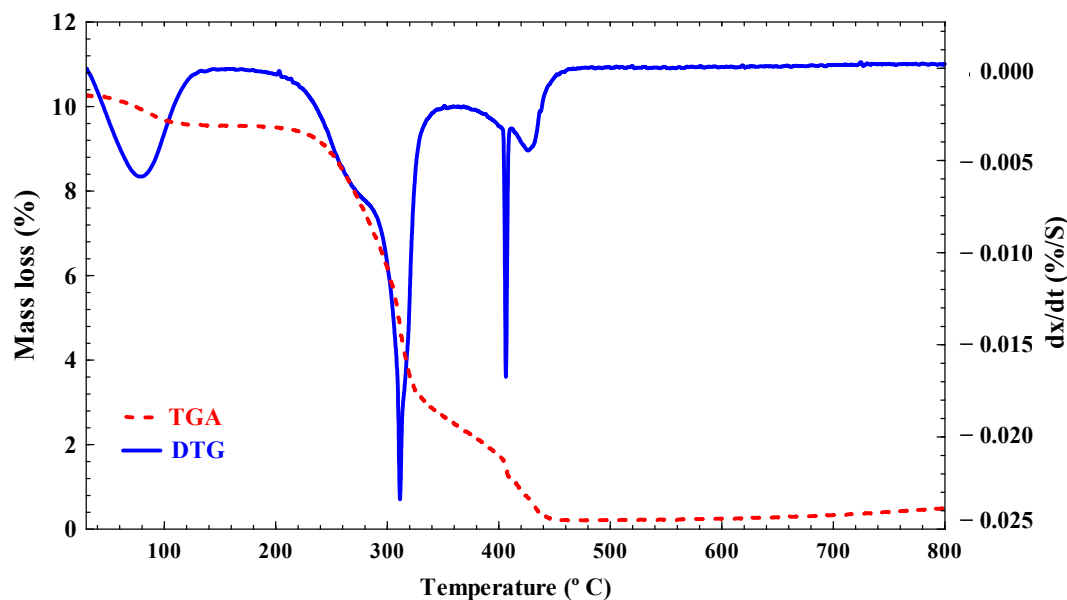
As indicated in Table 2, the lignocellulose composition showed that cellulose is the highest component followed by hemicellulose and lignin with values of 37.50%, 27.80%, and 18.40%, respectively. Cellulose would have contributed positively to the forming of micropores in the resulting activated carbon and increased the opportunity to produce activated carbon with high porosity. The proximate analysis indicated high volatile content (86.70%). The volatile matter would greatly contribute to the porosity formation in the ultimate product (active carbon) during the carbonization of biomass stuffs. The ultimate analysis showed a high carbon content (44.82%) that can increase the potency toward high fixed carbon [33].

Table 2. Wheat straw analysis data.

Analysis ^(a)	Element	Value (%)
Lignocellulose composition	Lignin	18.40
	Cellulose	37.50
	Hemicellulose	27.80
Proximate analysis	Moisture	7.12
	Ash	10.41
	Volatiles	86.70
Ultimate analysis	C	44.82
	H	7.32
	N	1.50

Note(s): ^(a) Based on dry weight except moisture content.

The TGA and DTG curves in an air atmosphere for the wheat straw sample have been detected to determine the thermal nature, as shown in Figure 3. The TGA curve indicated the mass loss in the sample. The initial weight loss was due to the drying moisture content, followed by a sharp decrease in the mass loss due to the high decomposition rate of straw, and finally small a mass loss was detected. The nature of the TGA curve in combination with the corresponding DTG peaks indicates the number of stages of thermal degradation. The DTG curve reveals three differentiated stages. The first peak in the burning profile, which occurs at temperatures below 100 °C, is corresponding to the drying stage; the second stage, corresponding to straw de-volatilization, begins over 200 °C, where the weight loss is due to decomposition and the emission of volatiles from cellulose and hemicellulose; and the third stage starts after 300 °C, and the weight loss correspond to lignin decomposition [34].

**Figure 3.** TGA/DTG for wheat straw sample.

The SEM inspection and related observations were conducted to determine the surface morphology of straw. Cavities (particularly void spaces in the cells) have been observed, as indicated in Figure 4. During the activation process, the cavities will act as media to distribute the activator into the carbon structure (impregnation) and concurrently release water vapor as well as gaseous matter. This condition will facilitate the porosity formation and produce activated carbon with high porosity [33].

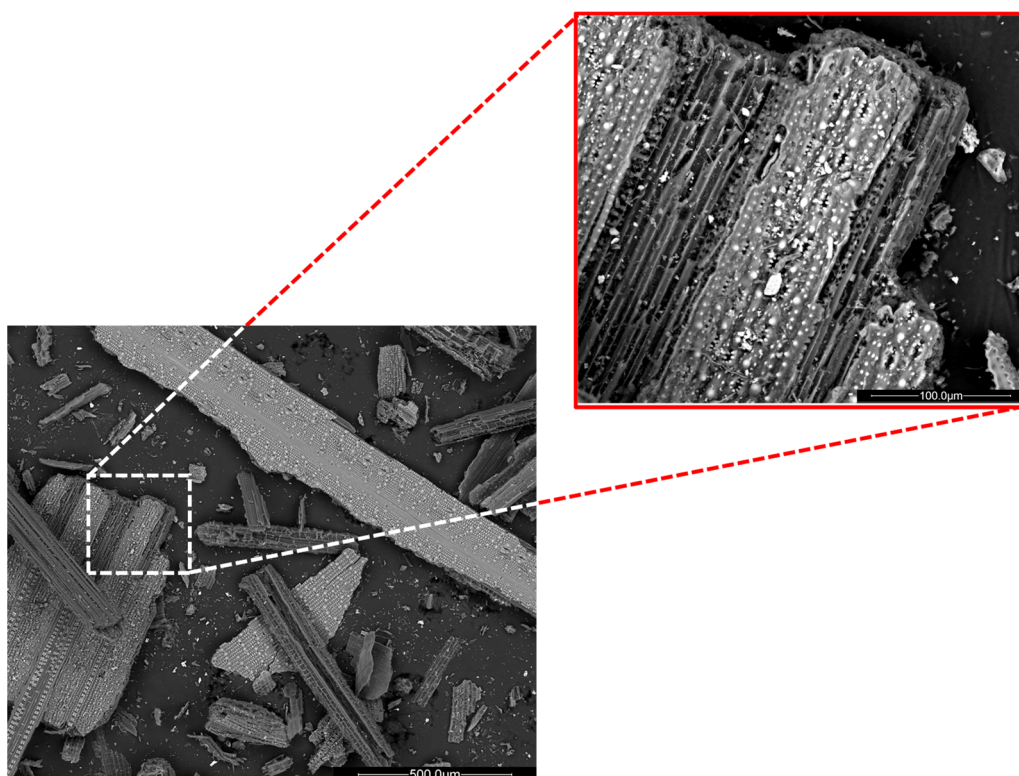


Figure 4. The SEM inspection for wheat straw sample at 500 μm and larger magnification at 100 μm .

3.2. Characteristics of Activated Carbons

Table 3 shows the textural and chemical characteristics of the used carbons ACWS and CACC. Both the ACWS and CACC carbons have a large surface area (1164 and 951 m^2/g , respectively) and large micro-pore volumes (W_0) obtained by N_2 adsorption (0.51 and 0.37 cm^3/g , respectively) and by CO_2 adsorption (0.48 and 0.22 cm^3/g , respectively). However, the ACWS has a higher surface area and larger micro-pore volume compared to the CACC. The pH of point of zero charge was 5.99 and 4.70 for carbons ACWS and CACC, respectively, which means that both carbons have a chemical nature acidic, which is due to the higher concentration of acidic groups (Table 3).

Table 3. Textural and chemical characteristics of activated carbons ACWS and CACC.

Carbon	S_{N_2} (a) (m^2/g)	W_0 (N_2) (b) (cm^3/g)	W_0 (CO_2) (c) (cm^3/g)	AGC (d) (meq/g)	BGC (e) (meq/g)	pH_{pzc} (f)
ACWS	1164	0.51	0.48	8712	3631	5.99
CACC	984	0.37	0.22	6290	0.0	4.70

Note(s): (a) Surface area. (b) Volumes of micropores (N_2). (c) Volumes of micropores (CO_2). (d) Acidic groups concentration. (e) Basic groups concentration. (f) pH of the point of zero charge.

Table 4 presents a comparison between the fabricated ACWS in the current study and other adsorbents in previous studies based on the used chemical agent, applied heating source, and surface area of ACs. As indicated in the table, the ACWS obtained in the current study showed a higher surface area than the other ACs fabricated from wheat straw and other biomass residues such as rice straw and corncob under conventional heating sources and using different chemical agents, which were obtained from previous studies. In contrast, the AC fabricated from wheat straw using a microwave as a source of heat showed a higher surface area than that obtained from the current study. However, using the microwave consumes more energy and leads to high-cost requirements. Thus, the

obtained ACWS in the current study has advantages compared to adsorbents in previous studies.

Table 4. Comparative between the fabricated ACWS in the current study and other adsorbents in previous studies.

Biomass Used for ACs	Chemical Agent	Heating	Surface Area (m ² /g)	Reference
Wheat straw (ACWS)	KOH	Conventional	1164	Current study
Wheat straw	ZnCl ₂	Conventional	907	[30]
Wheat straw	KOH	Conventional	552	[30]
Wheat straw	KOH	Microwave	1250	[29]
Rice straw	ZnCl ₂	Conventional	771	[11]
Rice straw	H ₃ PO ₄	Conventional	613	[11]
Corn cob	H ₃ PO ₄	Conventional	658	[26]

3.3. Adsorption Kinetics

Figure 5 presents the adsorption kinetics of the first-order and second-order kinetic models. Moreover, Table 5 represents the values of the adsorption kinetic models' constants that were calculated by using Statistica software (release 7). By using equation (3), the %D was calculated. The second-order kinetic model fitted the experimental data better than that for the first-order kinetic model with lower %D for both carbons except in the case of 100 mg of ACWS, where the %D was close to the first order (Table 5). Moreover, the theoretical maximum adsorption at equilibrium calculated by the second-order model was in agreement with the experimental data. Furthermore, by increasing the carbon mass, the kinetic constants for most of the experiments increased. This means that the adsorption rate increases by increasing the amount of carbon material [2,35].

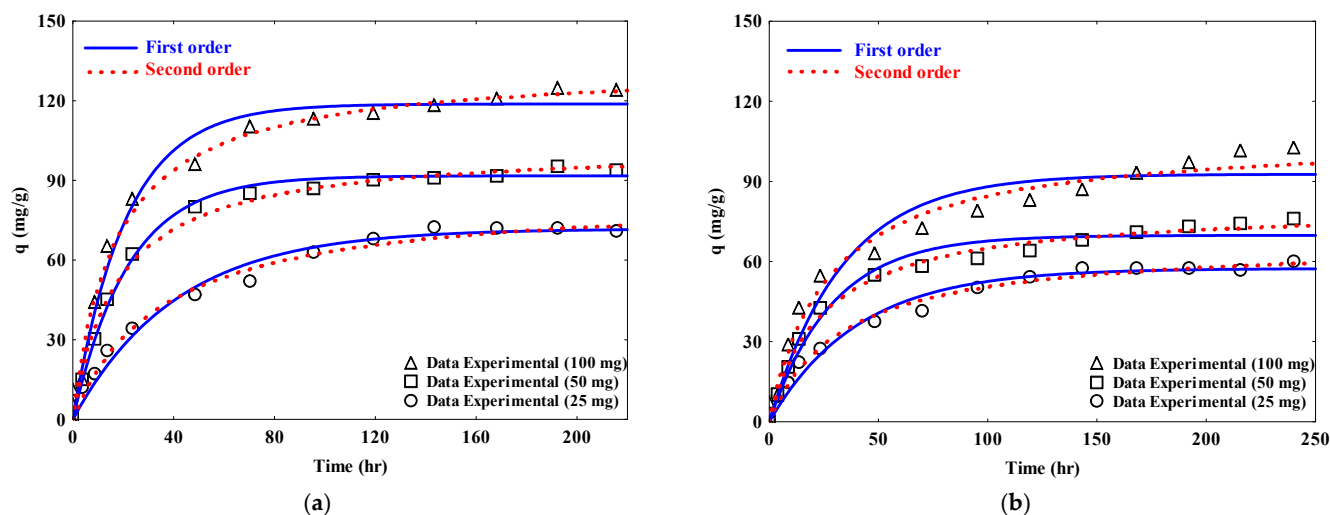


Figure 5. Adsorption kinetics of DPA onto (a) ACWS and (b) CACC at $[C]_0 = 100$ mg/L, $T = 25$ °C, $pH \approx 5$ and at 25 mg (○), 50 mg (□), and 100 mg (Δ).

Table 5. Adsorption kinetics data of DPA on activated carbons ACWS and CACC after applying the first and second-order models.

Carbon	Mass (mg)	q_e (exp.) (mg/g)	First-Order			Second-Order		
			$q_{pred,1}$ (mg/g)	$k_1 \times 10^{-2}$ (L/h)	%D	$q_{pred,2}$ (mg/g)	$k_2 \times 10^{-4}$ (g/mg/h)	%D
ACWS	25.00	72.65	71.79	2.43	19.69	84.85	3.37	16.27
	50.00	95.35	91.74	4.56	6.98	103.03	5.53	5.86
	100.00	124.74	118.79	4.79	18.24	133.30	4.46	18.49
CACC	25.00	60.03	57.39	2.47	20.61	59.23	4.42	16.68
	50.00	75.98	69.80	3.45	11.94	80.68	5.11	7.01
	100.00	102.35	92.71	2.98	21.32	107.05	3.51	18.58

3.4. Adsorption Isotherms

Figure 6 depicts the adsorption isotherms of DPA at $T = 25\text{ }^\circ\text{C}$ and $\text{pH} (4.90)$ on both carbon samples. Both adsorption isotherms showed L-behavior agreeing with Giles classification [36,37], which means that the ratio between the remaining DPA's concentration in the solution and the adsorbed portion on the carbon is reduced when the DPA concentration increases, yielding a concave curve. Moreover, it confirmed a high affinity between the adsorbate molecules and the adsorbent surface. Finally, it also confirmed that the two aromatic rings associated with the DPA were adsorbed parallel to the activated carbon surface [5].

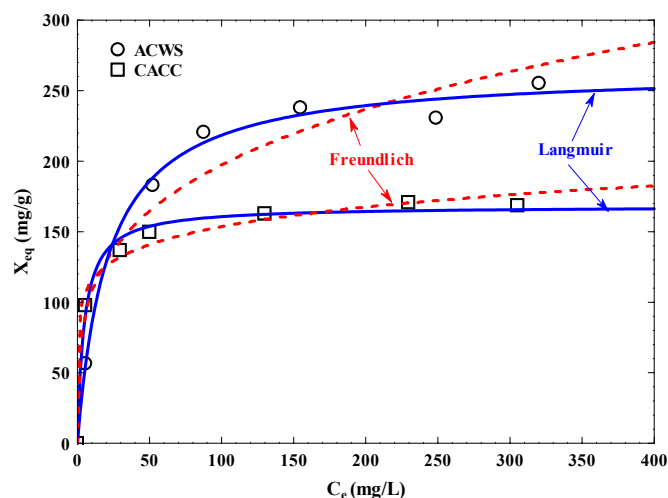
**Figure 6.** Adsorption isotherm of DPA onto ACWS (○) and CACC (□) at $T = 25\text{ }^\circ\text{C}$, $\text{pH} \approx 5$ and carbon mass 100 mg.

Table 6 indicates the comparison between the parameters obtained by applying the Langmuir and Freundlich isotherm models on the experiment data. The Langmuir model fitted the experiment data on the ACWS slightly better than the Freundlich model. However, the Freundlich model fitted the experiment data on CACC better than the Langmuir model. This means that the adsorption mechanism of the DPA on the ACWS was a monolayer, though it was a multilayer on CACC. This is confirmed by the adsorption capacity (X_m) of the ACWS (264.90 mg/g), which was higher than that of the CACC (168.19 mg/g). The adsorption capacity of carbons per area ($X'm$) was found to be higher with the ACWS than that with the CACC for the DPA, see Table 6,. This is due to the high surface area of the ACWS compared to that of the CACC. The adsorbent–adsorbate relative affinity (BX_m) obtained for the ACWS and CACC was 12.45 L/g and 35.99 L/g, respectively. This is consistent with that has been previously reported for the adsorption of aromatic

compounds [38]. However, the relative adsorption capacity (KF) of the DPA was higher on the CACC (86.51 L/g) than that on the ACWS (58.73 L/g); nevertheless, the ACWS has a higher surface area than the CACC. This confirms that the adsorption mechanism of the DPA on the CACC was a multilayer mechanism, whereas it was a monolayer mechanism on the ACWS.

Table 6. Parameters calculated by applying the Langmuir and Freundlich isotherm models of DPA adsorption isotherms onto ACWS and CACC.

Isotherm Model	Constants	ACWS	CACC
Langmuir	$X_m^{(a)}$ (mg/g)	264.90	168.19
	B ^(b) (L/mg)	0.047	0.214
	$BX_m^{(c)}$ (L/g)	12.45	35.99
	X'_m (mg/m ² /g)	0.23	0.17
	%D	2.52	2.73
Freundlich	$K_F^{(d)}$ (L/g)	58.73	86.51
	$1/n_F^{(e)}$	0.26	0.12
	%D	7.03	2.41

Note(s): ^(a) X_m : Adsorption capacity, (mg/g). ^(b) B: Langmuir constant, (L/mg). ^(c) BX_m : Adsorbent–adsorbate relative affinity, (L/g). ^(d) K_F : Relative adsorption capacity, (L/g). ^(e) $1/n_F$: Sorption intensity or surface heterogeneity.

3.5. Operational Parameters

Figure 7 shows the influence of the solution pH on the adsorption of the DPA onto both carbon materials, showing the significant effect of the solution pH. Thus, the adsorption capacity was improved at the acidic pH. The adsorption capacity of the ACWS is markedly decreased with a higher solution pH up to 6 and then remained virtually constant at higher solution pH values above 6. However, the CACC has a higher adsorption capacity at a solution pH around 5 compared to the rest of the solution pH. Both carbons have a negative charge density at a solution pH higher than 5.99 and 4.70 for the ACWS and CACC, respectively. The species distribution of the DPA has a negative charge density at a pH higher than 4.66. This means that the adsorbent–adsorbate electrostatic interactions play a major role in the adsorption process on the ACWS and are affected by the solution pH, and depend on the pH_{pzc} of the carbon and the species distribution of the DPA.

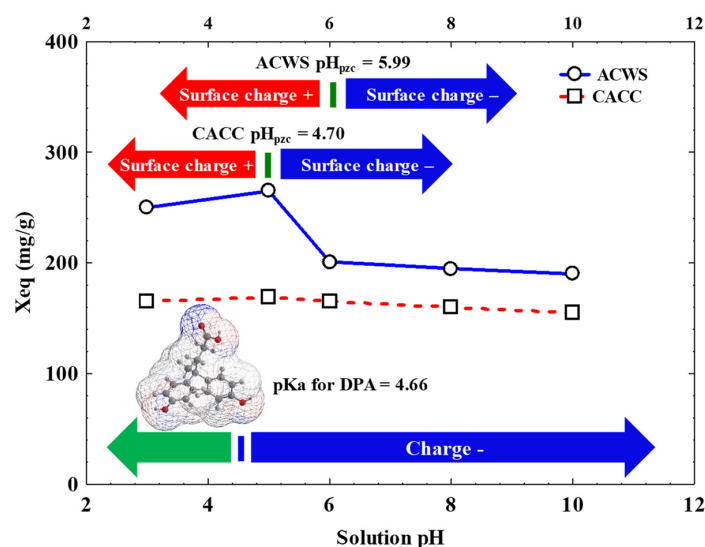


Figure 7. Influence of solution pH on the adsorption of DPA on ACWS (○) and CACC (□) at $T = 25\text{ }^{\circ}\text{C}$ and $[C]_0 = 500\text{ mg/L}$.

Figure 8 represents the results of the adsorption of the DPA on the carbon samples in the presence of NaCl ions at a pH of around 5. As shown, the presence of ionic strength in the solution had no influence on DPA removal. A slight increase in DPA adsorption was detected with the presence of NaCl ions. This is explained by the positive net charge of the molecular form of DPA and the carbon at the solution pH around 5. The presence of NaCl ions therefore favors adsorbent–adsorbate dispersive interactions through a screening effect [5].

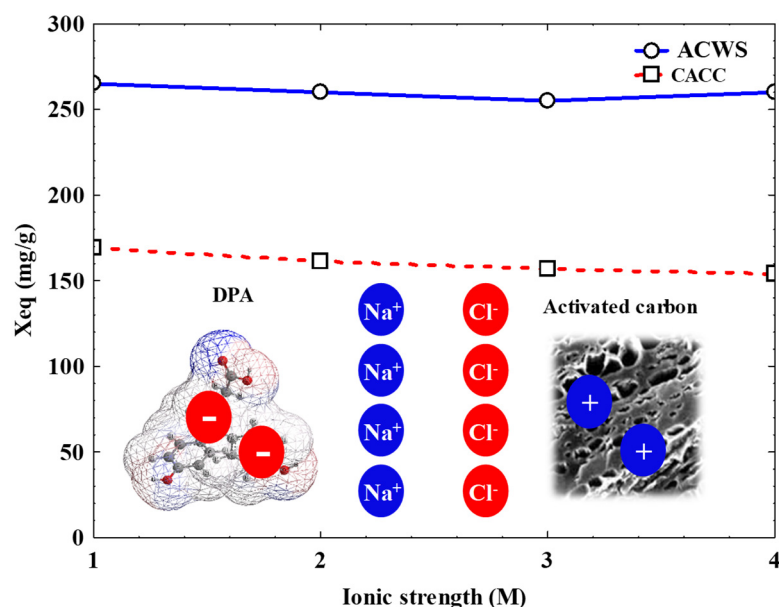


Figure 8. Influence of ionic strength on the adsorption of DPA on ACWS (○) and CACC (□) at $T = 25\text{ }^{\circ}\text{C}$, $\text{pH} \approx 5.00$, and $[\text{C}]_0 = 500\text{ mg/L}$.

Thus, the ACWS is an effective material for the adsorption of DPA at different solution pH; however, the highest adsorption yield was recorded for the acidic solution (pH 5). Moreover, the recycling of the saturated ACs is very important from an environmental point of view for safe disposal or reuse due to stringent environmental regulations. The regeneration of the saturated ACs can be conducted by various physical or chemical techniques with the objective of restoring the original porous structure with no damage [25].

4. Conclusions

The adsorption of diphenolic acid (DPA) was investigated on ACWS and CACC via adsorption kinetics and isotherms. Moreover, the influence of the solution pH and the ionic strength on the adsorption capacity of the DPA on both carbons were analyzed. The results showed that both the ACWS and CACC carbons have a large surface area (1164 and $951\text{ m}^2/\text{g}$, respectively) and large micro-pore volumes (W_0) obtained by N_2 (0.51 and $0.37\text{ cm}^3/\text{g}$, respectively) and by CO_2 adsorption (0.48 and $0.22\text{ cm}^3/\text{g}$, respectively). The second-order kinetics model fitted the experiment data better than the first kinetics models, with a lower %D. The adsorption capacity of the ACWS (264.90 mg/g) is higher than that of the CACC (168.19 mg/g) because of the higher surface area and volume of micropores of the ACWS. The adsorption isotherm showed that the adsorption of the DPA on the ACWS and CACC was consistent with the Langmuir and Freundlich isotherm models, respectively. The solution pH had a major effect on DPA adsorption on both carbons; moreover, the adsorption process is favored at the acidic pH but was not affected by the presence of electrolytes in the solution. These findings support the use of wheat straw-activated carbon for DPA adsorption. Moreover, it could be used to adsorb other similar contaminants from aqueous solution and from other water types (surface and groundwater, and municipal and industrial wastewater). Thus, the conversion of wheat straw to activated carbon and

its utilization as an adsorbent can possibly help to solve the problems of pollution caused by DPA in aqueous phase and straw open burning.

Author Contributions: All authors whose names appear on the submission made substantial contributions. Conceptualization, R.A., N.S. and M.M.A.D.; methodology, R.A., N.S. and M.M.A.D.; analysis, R.A., N.S., M.T.B., A.G., B.A. and M.M.A.D. The first draft of the manuscript was written by N.S. and M.M.A.D.; revised and presented suggestive comments about the previous versions of the manuscript, R.A., N.S., M.T.B., A.G., B.A. and M.M.A.D. All authors have read and agreed to the published version of the manuscript.

Funding: This work was funded by the Deanship of Scientific Research at Jouf University under grant number DSR2022-RG-0106.

Data Availability Statement: Data for this work can be found within the article, and for further data feel free to contact the corresponding authors.

Acknowledgments: The authors extend their appreciation to the Deanship of Scientific Research at Jouf University for financial support through Research Support Program (DSR2022-RG-0106).

Conflicts of Interest: The authors confirm that there is no conflict concerning the publication of this manuscript.

References

1. Evode, N.; Qamar, S.A.; Bilal, M.; Barceló, D.; Iqbal, H.M.N. Plastic waste and its management strategies for environmental sustainability. *Case Stud. Chem. Environ. Eng.* **2021**, *4*, 100142. [[CrossRef](#)]
2. Ocampo-Perez, R.; Rivera-Utrilla, J.; Abdel daiem, M.M.; Sánchez-Polo, M. *Integrated Technologies Based on the Use of Activated Carbon and Radiation to Remove Contaminants Present in Landfill Leachates*; Nova Science Publishers, Inc.: New York, NY, USA, 2015; ISBN 9781634638241.
3. Khasawneh, O.F.S.; Palaniandy, P.; Kamaruddin, M.A.; Aziz, H.A.; Hung, Y.-T. Landfill Leachate Collection and Characterization. In *Solid Waste Engineering and Management*; Springer: Berlin/Heidelberg, Germany, 2022; pp. 599–657.
4. Rivera-Utrilla, J.; Abdel daiem, M.M.; Sánchez-Polo, M.; Ocampo-Pérez, R.; López-Peñalver, J.J.; Velo-Gala, I.; Mota, A.J. Removal of compounds used as plasticizers and herbicides from water by means of gamma irradiation. *Sci. Total Environ.* **2016**, *569–570*, 518–526. [[CrossRef](#)] [[PubMed](#)]
5. Abdel daiem, M.M.; Rivera-Utrilla, J.; Sánchez-Polo, M.; Ocampo-Pérez, R. Single, competitive, and dynamic adsorption on activated carbon of compounds used as plasticizers and herbicides. *Sci. Total Environ.* **2015**, *537*, 335–342. [[CrossRef](#)]
6. Abdel Daiem, M.M.; Rivera-Utrilla, J.; Ocampo-Pérez, R.; Sánchez-Polo, M.; López-Peñalver, J.J. Treatment of water contaminated with diphenolic acid by gamma radiation in the presence of different compounds. *Chem. Eng. J.* **2013**, *219*, 371–379. [[CrossRef](#)]
7. Cerbai, B.; Solaro, R.; Chiellini, E. Synthesis and characterization of functional polyesters tailored for biomedical applications. *J. Polym. Sci. Part A Polym. Chem.* **2008**, *46*, 2459–2476. [[CrossRef](#)]
8. Auf'mkolk, M.; Köhrle, J.; Gumbinger, H.; Winterhoff, H.; Hesch, R.-D. Antihormonal effects of plant extracts: Iodothyronine deiodinase of rat liver is inhibited by extracts and secondary metabolites of plants. *Horm. Metab. Res.* **1984**, *16*, 188–192. [[CrossRef](#)]
9. Guo, L.; Wang, B.; Huang, W.; Wu, F.; Huang, J. Photocatalytic degradation of diphenolic acid in the presence of beta-cyclodextrin under UV light. In Proceedings of the 2009 International Conference on Environmental Science and Information Application Technology, Wuhan, China, 4–5 July 2009; IEEE: Piscataway Township, NJ, USA, 2009; Volume 3, pp. 322–324.
10. Guo, Z.; Dong, Q.; He, D.; Zhang, C. Gamma radiation for treatment of bisphenol A solution in presence of different additives. *Chem. Eng. J.* **2012**, *183*, 10–14. [[CrossRef](#)]
11. Abdel daiem, M.M.; Sánchez-Polo, M.; Rashed, A.S.; Kamal, N.; Said, N. Adsorption mechanism and modelling of hydrocarbon contaminants onto rice straw activated carbons. *Pol. J. Chem. Technol.* **2019**, *21*, 1–12. [[CrossRef](#)]
12. Abdel daiem, M.M.; Rashad, A.M.; Said, N.; Abdel-Gawwad, H.A. An initial study about the effect of activated carbon nano-sheets from residual biomass of olive trees pellets on the properties of alkali-activated slag pastes. *J. Build. Eng.* **2021**, *44*, 102661. [[CrossRef](#)]
13. Abdel daiem, M.; Alotaibi, A.A.A.; Alosime, E.M.E.M.; Zaidi, B.; Said, N. Structural-property relationship in activated carbon synthesized from rice straw for electronic application. *Pol. J. Environ. Stud.* **2020**, *29*, 3535–3547. [[CrossRef](#)]
14. García-Mateos, F.J.; Ruiz-Rosas, R.; Marqués, M.D.; Cotoruelo, L.M.; Rodríguez-Mirasol, J.; Cordero, T. Removal of paracetamol on biomass-derived activated carbon: Modeling the fixed bed breakthrough curves using batch adsorption experiments. *Chem. Eng. J.* **2015**, *279*, 18–30. [[CrossRef](#)]
15. Sun, Z.; Wang, M.; Fan, J.; Zhou, Y.; Zhang, L. Regeneration performance of activated carbon for desulfurization. *Appl. Sci.* **2020**, *10*, 6107. [[CrossRef](#)]
16. Gan, Y.X. Activated carbon from biomass sustainable sources. *Carbon* **2021**, *7*, 39. [[CrossRef](#)]

17. Abdel daiem, M.M.; Said, N. Assessment and Contribution of Biomass Residues to Renewable Energy Resources in Egypt. In *The Handbook of Environmental Chemistry*; Springer: Berlin/Heidelberg, Germany, 2023; pp. 1–28.
18. Abdel Daiem, M.M.; Said, N. Energetic, economic, and environmental perspectives of power generation from residual biomass in Saudi Arabia. *Alex. Eng. J.* **2022**, *61*, 3351–3364. [[CrossRef](#)]
19. Singh, P.K.; Mohanty, P.; Mishra, S.; Adhya, T.K. Food Waste Valorisation for Biogas-Based Bioenergy Production in Circular Bioeconomy: Opportunities, Challenges, and Future Developments. *Front. Energy Res.* **2022**, *10*, 903775. [[CrossRef](#)]
20. Abdel Daiem, M.M.; Said, N.; Negm, A.M. Potential energy from residual biomass of rice straw and sewage sludge in Egypt. *Procedia Manuf.* **2018**, *22*, 818–825. [[CrossRef](#)]
21. Sánchez-Polo, M.; Rivera-Utrilla, J.; Ocampo-Perez, R.; López-Penalver, J.J.; Velo-Gala, L.; Abdel Daiem, M.M. *Degradation of Emerging Aromatic Micropollutants by UV-Based Oxidation Processes*; Nova Science Publishers, Inc.: New York, NY, USA, 2014; ISBN 9781633210936.
22. Wang, H.; Xu, J.; Liu, X.; Sheng, L. Preparation of straw activated carbon and its application in wastewater treatment: A review. *J. Clean. Prod.* **2021**, *283*, 124671. [[CrossRef](#)]
23. Ani, J.U.; Akpomie, K.G.; Okoro, U.C.; Aneke, L.E.; Onukwuli, O.D.; Ujam, O.T. Potentials of activated carbon produced from biomass materials for sequestration of dyes, heavy metals, and crude oil components from aqueous environment. *Appl. Water Sci.* **2020**, *10*, 1–11. [[CrossRef](#)]
24. Januszewicz, K.; Kazimierski, P.; Klein, M.; Kardaś, D.; Łuczak, J. Activated carbon produced by pyrolysis of waste wood and straw for potential wastewater adsorption. *Materials* **2020**, *13*, 2047. [[CrossRef](#)]
25. Hwang, S.Y.; Lee, G.B.; Kim, J.H.; Hong, B.U.; Park, J.E. Pre-Treatment methods for regeneration of spent activated carbon. *Molecules* **2020**, *25*, 4561. [[CrossRef](#)]
26. Feng, P.; Li, J.; Wang, H.; Xu, Z. Biomass-based activated carbon and activators: Preparation of activated carbon from corncob by chemical activation with biomass pyrolysis liquids. *ACS Omega* **2020**, *5*, 24064–24072. [[CrossRef](#)] [[PubMed](#)]
27. Gayathiri, M.; Pulingam, T.; Lee, K.T.; Sudesh, K. Activated carbon from biomass waste precursors: Factors affecting production and adsorption mechanism. *Chemosphere* **2022**, *294*, 133764. [[CrossRef](#)] [[PubMed](#)]
28. Ministry of Environment Water and Agriculture MEWA. Available online: [https://en.wikipedia.org/wiki/Ministry_of_Environment,_Water,_and_Agriculture_\(Saudi_Arabia\)](https://en.wikipedia.org/wiki/Ministry_of_Environment,_Water,_and_Agriculture_(Saudi_Arabia)) (accessed on 2 January 2023).
29. Mao, H.; Zhou, D.; Hashisho, Z.; Wang, S.; Chen, H.; Wang, H.H.; Lashaki, M.J. Microporous activated carbon from pinewood and wheat straw by microwave-assisted KOH treatment for the adsorption of toluene and acetone vapors. *RSC Adv.* **2015**, *5*, 36051–36058. [[CrossRef](#)]
30. Ma, Y. Comparison of activated carbons prepared from wheat straw via ZnCl₂ and KOH activation. *Waste Biomass Valorization* **2017**, *8*, 549–559. [[CrossRef](#)]
31. Abdel daiem, M.M.; Hatata, A.; Said, N. Modeling and optimization of semi-continuous anaerobic co-digestion of activated sludge and wheat straw using Nonlinear Autoregressive Exogenous neural network and seagull algorithm. *Energy* **2022**, *241*, 122939. [[CrossRef](#)]
32. Méndez-Díaz, J.D.; Abdel daiem, M.M.; Rivera-Utrilla, J.; Sánchez-Polo, M.; Bautista-Toledo, I. Adsorption/bioadsorption of phthalic acid, an organic micropollutant present in landfill leachates, on activated carbons. *J. Colloid Interface Sci.* **2012**, *369*, 358–365. [[CrossRef](#)]
33. Darmawan, S.; Wistara, N.J.; Pari, G.; Maddu, A.; Syafii, W. Characterization of Lignocellulosic Biomass as Raw Material for the Production of Porous Carbon-based Materials. *BioResources* **2016**, *11*, 3561–3574. [[CrossRef](#)]
34. Said, N.; Bishara, T.; García-Maraver, A.; Zamorano, M. Effect of water washing on the thermal behavior of rice straw. *Waste Manag.* **2013**, *33*, 2250–2256. [[CrossRef](#)]
35. Rivera-Utrilla, J.; Gómez-Pacheco, C.V.; Sánchez-Polo, M.; López-Peñalver, J.J.; Ocampo-Pérez, R. Tetracycline removal from water by adsorption/bioadsorption on activated carbons and sludge-derived adsorbents. *J. Environ. Manag.* **2013**, *131*, 16–24. [[CrossRef](#)]
36. Giles, C.H.; Smith, D.; Huitson, A. A general treatment and classification of the solute adsorption isotherm. I. Theoretical. *J. Colloid Interface Sci.* **1974**, *47*, 755–765. [[CrossRef](#)]
37. Barton, P.I.; Pantelides, C.C. Modeling of combined discrete/continuous processes. *AIChE J.* **1994**, *40*, 966–979. [[CrossRef](#)]
38. Radovic, L.R.; Moreno-Castilla, C.; Rivera-Utrilla, J. Carbon materials as adsorbents in aqueous solutions. *Chem. Phys. Carbon* **2001**, *27*, 227–406.

Disclaimer/Publisher’s Note: The statements, opinions and data contained in all publications are solely those of the individual author(s) and contributor(s) and not of MDPI and/or the editor(s). MDPI and/or the editor(s) disclaim responsibility for any injury to people or property resulting from any ideas, methods, instructions or products referred to in the content.